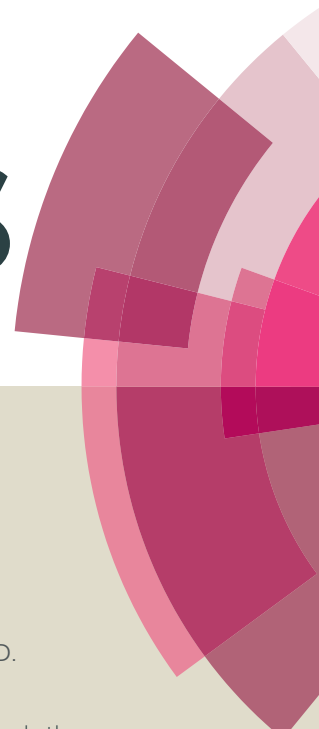


RSC Advances



This article can be cited before page numbers have been issued, to do this please use: A. V. Müller, L. D. Ramos, K. Frin, K. T. de Oliveira and A. S. Polo, *RSC Adv.*, 2016, DOI: 10.1039/C6RA08666G.



This is an *Accepted Manuscript*, which has been through the Royal Society of Chemistry peer review process and has been accepted for publication.

Accepted Manuscripts are published online shortly after acceptance, before technical editing, formatting and proof reading. Using this free service, authors can make their results available to the community, in citable form, before we publish the edited article. This *Accepted Manuscript* will be replaced by the edited, formatted and paginated article as soon as this is available.

You can find more information about *Accepted Manuscripts* in the [Information for Authors](#).

Please note that technical editing may introduce minor changes to the text and/or graphics, which may alter content. The journal's standard [Terms & Conditions](#) and the [Ethical guidelines](#) still apply. In no event shall the Royal Society of Chemistry be held responsible for any errors or omissions in this *Accepted Manuscript* or any consequences arising from the use of any information it contains.

High efficiency ruthenium(II) *tris*-heteroleptic dye containing 4,7-dicarbazole-1,10-phenanthroline for nanocrystalline solar cells

Andressa V. Müller^a, Luiz D. Ramos^a, Karina P. M. Frin^a, Kleber T. de Oliveira^b, André S. Polo^{*a}

Received 00th January 20xx,
Accepted 00th January 20xx

DOI: 10.1039/x0xx00000x

www.rsc.org/

The *tris*-heteroleptic polypyridyl ruthenium(II) dye, *cis*-[Ru(cbz₂-phen)(dcbH₂)(NCS)₂], cbz₂-phen = 4,7-dicarbazole-1,10-phenanthroline and dcbH₂ = 4,4'-dicarboxylic acid 2,2'-bipyridine, was designed, synthesized, purified via liquid chromatography and characterized using ¹H NMR, FTIR, cyclic voltammetry, absorption and emission spectra. The compound exhibits broad and intense MLCT bands that overlap the visible spectrum and it is capable of sensitizing TiO₂ films. The energy levels of *cis*-[Ru(cbz₂-phen)(dcbH₂)(NCS)₂] are adequate for its use in DSSCs. The solar cells prepared using this dye achieved a performance that surpasses the N3 one under the same conditions. The introduction of extended π-conjugated carbazole substituent at the 4 and 7 positions of 1,10-phenanthroline increases the IPCE and the overall solar cell efficiency. This high performance is ascribed to the HOMO stabilization and to the increase in electron delocalization of the triplet excited state, which favors the electron injection via singlet and triplet pathways.

INTRODUCTION

Solar energy conversion is a meaningful alternative for producing renewable energy to help solve the environmental and energetic issues of the world because solar energy is clean, plentiful and inexhaustible. A major harnessing strategy of solar energy is its direct conversion into electrical output. Among the photovoltaic devices that have been developed over the past decades, Dye-Sensitized Solar Cells (DSSCs) stand out due to their low cost, good power conversion efficiency, easy fabrication and low sensitivity to temperature changes.¹⁻⁶ The DSSCs are photoelectrochemical devices that are based on a wide band-gap semiconductor with a mesoporous nanocrystalline morphology, typically TiO₂. The semiconductor is sensitized with a light-harvesting dye, in which optical absorption is followed by a photoinduced electron injection from the dye into the TiO₂ conduction band.⁷ Improvement of semiconductor⁸⁻¹⁴ or redox mediator¹⁵⁻²⁰ has been the focus of several publications. However, the development of more efficient dye-sensitizers is also a key aspect for advancing these devices because dye-sensitizers are responsible for initiating the photoelectrochemical energy conversion processes by absorbing photons and subsequently transferring electrons. Several groups have developed organic

and metal-based dyes that aim to increase the performance of DSSCs.²¹⁻³⁰ However, just a few devices have achieved higher efficiencies than those obtained by the Ru(II) complexes based DSSCs.

Due to the outstanding performance of the N3 dye and its double-deprotonated analogous N719, the efforts have been concentrated on the design of new *cis*-[Ru(LL)(dcbH₂)(NCS)₂] dyes, dcbH₂ = 2,2'-bipyridine-4,4'-dicarboxylic acid and LL = polypyridyl ancillary ligands. Ruthenium(II) *tris*-heteroleptic compounds with amphiphilic derivatives of 2,2'-bipyridine showed long-term stability. However, molar absorptivities similar to those determined for N3 or N719 resulted in a lower photoelectrochemical performance compared with N3.³¹⁻³⁴ The complexes prepared with donor-antenna substituent derivatives of 2,2'-bipyridine were designed to improve light absorption and to enhance the hydrophobic character of the dye.^{35, 36} The use of aromatic substituents can promote this effect because aromaticity increases light absorption. Furthermore, the existence of a hydrophobic chain protects the dye from desorbing by water.³⁶

Few papers have reported the use of 1,10-phenanthroline and their derivatives as ancillary ligands.³⁷⁻⁴⁴ Its extended π-conjugated structure and similarity to the 2,2'-bipyridine ligand leads to favorable properties for the energy conversion processes.³⁷ The first compound developed for DSSCs that has 1,10-phenanthroline as an ancillary ligand demonstrated its potential as a new class of sensitizers. However, the devices did not exhibit better performance than N3.³⁸ The insertion of different substituents at some positions of phenanthroline cores can either improve or decrease the performance of devices. This may be ascribed to interfacial electron recombination dynamics.^{45, 46} However, the Y55 complex, which is based on 4,7-diphenyl-1,10-phenanthroline, exhibits

^a Centro de Ciências Naturais e Humanas, Universidade Federal do ABC - UFABC, Av dos Estados, 5001, 09210-580, Santo André - SP, Brazil

^b Departamento de Química, Universidade Federal de São Carlos - UFSCAR, Rodovia Washington Luis, km 235, 13565-905, São Carlos - SP, Brazil
Electronic Supplementary Information (ESI) available: ¹H NMR, ¹³C{¹H} NMR and DEPT-135 ¹³C NMR spectra of cbz₂-phen; ¹H NMR and ¹H-¹H COSY spectra of *cis*-[Ru(cbz₂-phen)(dcbH₂)(NCS)₂]; absorption spectra of TiO₂ film during sensitizing by *cis*-[Ru(cbz₂-phen)(dcbH₂)(NCS)₂]; absorption spectra of *cis*-[Ru(phen)(dcbH₂)(NCS)₂] in ethanol. See DOI: 10.1039/x0xx00000x

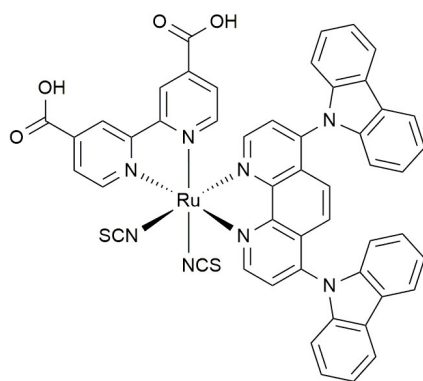


Figure 1. Structure of *cis*-[Ru(cbz₂-phen)(dcbH₂)(NCS)₂].

high molar absorptivity and a comparable to N719 performance under the same experimental conditions. This indicates that the high-conjugated substituents attached to 1,10-phenanthroline rings is a good strategy for improving molar absorptivity of the complex. This makes these compounds interesting to investigate.⁴¹

Specifically, the introduction of two aromatic groups at the 4 and 7 positions of the 1,10-phenanthroline ring can increase molar absorptivity of the sensitizer and directly result in higher photocurrent generation and in the overall solar cell efficiency. Furthermore, insertion of a bulky substituent decreases the mediator concentration in the vicinity of TiO₂, which harms the semiconductor-electrolyte recombination dynamics.⁴⁷ In this context, carbazole is a potential substituent that has already demonstrated improvements in the stability and light-harvesting capacity of 2,2'-bipyridine-based Ru(II) dyes.⁴⁸⁻⁵⁰ Herein, we report the synthesis, characterization and photoelectrochemical performance of the novel *tris*-heteroleptic ruthenium(II) *cis*-[Ru(cbz₂-phen)(dcbH₂)(NCS)₂], cbz₂-phen = 4,7-dicarbazole-1,10-phenanthroline and dcbH₂ = 4,4'-dicarboxylic acid 2,2'-bipyridine, Figure 1, as a dye-sensitizer for solar cells.

EXPERIMENTAL

Materials

The materials and reagents were used as received from the indicated commercial suppliers: 4,4'-dimethyl-2,2'-bipyridine (Aldrich, 99%), H₂SO₄ (Sigma-Aldrich, 97%), Na₂Cr₂O₇ (Synth, 99.5%), NaOH (Sigma-Aldrich, >98%), HCl (Synth, 36.5%), carbazole (Aldrich, ≥95%), potassium *tert*-butoxide (Aldrich, ≥98%), 4,7-dichloro-1,10-phenanthroline (Aldrich, 97%), tetrahydrofuran (THF; Synth, 99.0%), toluene (Synth, 99.5%), ethyl acetate (Synth, 99.5%), silica (Sigma-Aldrich, ≥98%), [Ru(*p*-cymene)Cl₂]₂ (Strem, 98%), NaNCS (Merck, 98.5%), N,N-dimethylformamide (DMF; Synth, 99.8%), methanolic solution of tetrabutylammonium hydroxide (TBAOH; Acros Organics, 1.0 mol L⁻¹), Sephadex LH-20 (Aldrich), HNO₃ (Sigma-Aldrich, 65%), methanol (Synth, 99.8%), N,N'-dimethylformamide-d₇,

(DMF-d₇; Cambridge, 99.5%), ethanol (Merck, Lichrosolv), acetonitrile (Merck, Lichrosolv), tetrabutylammonium hexafluorophosphate (TBAPF₆; Fluka, ≥99.0%, electrochemical grade), ferrocene (Fc; Aldrich, 98%), isopropanol (Synth, 99.5%), hexachloroplatinic acid (H₂PtCl₆; Acros), TiCl₄ standard aqueous solution (Sigma-Aldrich, 1.00 g L⁻¹, standard solution), transparent 20 nm TiO₂ anatase nanoparticles paste (18NR-T, Dyesol), fluorine-doped SnO₂-coated glass (FTO; Aldrich, 3.2 mm thick, 8 Ω/□), low temperature sealant - Surlyn (30 μm - Dyesol), valeronitrile (Aldrich, 99.5%), iodine (Sigma-Aldrich, ≥99.8%), guanidine thiocyanate (Sigma-Aldrich, ≥97%), 4-*tert*-butylpyridine (Aldrich, 96%) and 1-butyl-3-methylimidazolium iodide (Aldrich, 98%). Additionally, *cis*-[Ru(phen)(dcbH₂)(NCS)₂] and *cis*-[Ru(dcbH₂)₂(NCS)₂], N3, were available from a previous study.⁴⁴

Synthesis of 2,2'-bipyridine-4,4'-dicarboxylic acid, dcbH₂

The compound 2,2'-bipyridine-4,4'-dicarboxylic acid (dcbH₂) was synthesized with slight modifications of the previously described procedure.^{43, 51} Briefly, 3.23 g (17.55 mmol) of 4,4'-dimethyl-2,2'-bipyridine was added to the solution of 11.80 g (39.6 mmol) of Na₂Cr₂O₇ that was dissolved in 45 mL of concentrated H₂SO₄, and the mixture was stirred for 30 min in an ice bath. The resulting solution was added to 410 mL of cold water, the solid was removed, and 50 mL of water was added. The solid was dissolved by adding 10% NaOH until pH 10. The final product was precipitated by adding 2.0 mol L⁻¹ HCl to the solution until it reached pH 2, and the white solid was collected. Yield: 93% *Anal.* Calc. for C₁₂H₈N₂O₄: C, 59.02; H, 3.30; N, 11.47%. Found: C, 58.21; H, 3.45; N, 11.09%.

Synthesis of 4,7-di(9H-carbazol-9-yl)-1,10-phenanthroline, cbz₂-phen

The compound was prepared with modifications of the previously described procedure.⁵²⁻⁵⁴ In a round bottom flask, 2.73 g (16.0 mmol) of carbazole and 1.95 g (16.0 mmol) of potassium *tert*-butoxide was added to dry THF (40 mL) under argon atmosphere, and the mixture was heated to reflux. After 1 h, 1.0 g (4.00 mmol) of 4,7-dichloro-1,10-phenanthroline was added, and the reflux was maintained for 24 h. The reaction was quenched with water (100 mL) and was extracted with toluene (3 × 100 mL). Organic layers were dried over anhydrous sodium sulfate, and the solvent was distilled off under reduced pressure. Purification was performed using column chromatography. Specifically, silica was used as a stationary phase, and toluene:ethyl acetate (gradient from 9:1 to 6:4) was used as an eluent. The fraction of interest was collected, the solvent was distilled off, and the solid was recrystallized from MeOH. Yield: (0.57 g, 1.1 mmol, 55%). *Anal.* Calc. for C₃₆H₂₂N₄: C, 84.68; H, 4.34; N, 10.97% Found: C, 84.55; H, 4.55; N, 10.76%. ¹H NMR (CDCl₃, 500 MHz, δ/ppm): 9.48 (d, 2H); 8.15 (d, 4H); 7.85 (d, 2H); 7.28-7.37 (m, 10H); 7.07 (d, 4H). ¹³C NMR (CDCl₃, 125 MHz, δ/ppm): 151.5 (CH); 148.7 (C); 143.3 (C); 141.2 (C); 126.5 (C); 126.4 (CH); 123.9 (C); 122.8 (CH); 120.6 (CH); 110.0 (CH).

Synthesis of *cis*-[Ru(cbz₂-phen)(dcbH₂)(NCS)₂]

The *cis*-[Ru(cbz₂-phen)(dcbH₂)(NCS)₂] complex was prepared using one-pot procedure that was previously reported for similar compounds.^{43, 44} Briefly, the ruthenium *p*-cymene dimer, [Ru(*p*-cymene)Cl₂]₂ (0.17 g, 0.27 mmol), was dissolved in 50 mL of *N,N'*-dimethylformamide and 0.28 g of cbz₂-phen (0.54 mmol) was added. The mixture was kept at 80 °C for 2 h under argon atmosphere. After this period, 0.13 g of dcbH₂ (0.54 mmol) was added to the mixture, and the temperature was increased to 160 °C and was kept at this level for 4 h. Finally, 0.44 g of NaNCS (5.4 mmol) was added, the temperature was decreased to 140 °C, and the reaction was kept under these conditions for 4 h, which allowed it to proceed to completion. The compound was purified by concentrating the obtained solution, washed and filtered with ultrapure H₂O, dissolved in a methanolic TBAOH solution (1.0 mol L⁻¹), centrifuged to remove any residual particles and loaded on a liquid column chromatography containing Sephadex LH-20 as the stationary phase and methanol as the eluent. The purification process was repeated 3 times. The main fraction was concentrated, precipitated by adding H₂SO₄ (0.5 mol L⁻¹) to reach pH ~ 1.0 and, finally, filtered. The obtained solid was dried in a vacuum oven and weighed 0.21 mg. Yield = 39%. *Anal.* Calc. for C₅₀H₃₆N₈O₇RuS₂: C, 58.53; H, 3.54; N, 10.92%. Found: C, 58.87; H, 3.37; N, 10.44%. ¹H NMR (DMF-d₇, 500 MHz, δ/ppm): 10.08 (d, J = 5.8 Hz; 1H); 9.90 (d, J = 6.0 Hz; 1H); 9.36 (s, 1H); 9.19 (s, 1H); 8.79 (d, J = 5.8 Hz; 1H); 8.60 (d, J = 5.8 Hz; 1H); 8.54 (d, J = 6.0 Hz; 1H); 8.41 (s, 1H); 8.40 (s, 1H); 8.28-8.32 (m, 4H); 8.01 (d, J = 5.8 Hz; 1H); 7.83 (d, J = 9.5 Hz; 1H); 7.71 (d, J = 9.5 Hz; 1H); 7.63-7.67 (m, 2H); 7.49-7.55 (m, 2H); 7.42-7.46 (m, 3H); 7.26-7.38 (m, 5H).

Methods

NMR spectra were recorded at 298 K using a DRX-500 Bruker Avance spectrometer at 500.13 MHz using DMF-d₇ as the solvent. The residual DMF peaks were used as the internal standard. All NMR spectra are presented in the supporting information. FTIR spectrum of the solid was recorded at 298 K in KBr pellets using a Bomem MB 100 spectrometer (4 cm⁻¹ resolution). The adsorbed TiO₂ film spectrum was registered using attenuated total reflectance (ATR) FTIR that was recorded at 298 K using a Perkin Elmer Spectrum Two spectrometer (4 cm⁻¹ resolution). Electronic absorption spectra were recorded in quartz cuvettes (1.000 cm path length) using an Agilent 8453 diode-array spectrophotometer. Emission spectra were recorded in quartz cuvettes (1.000 cm path length) using a Cary Eclipse spectrofluorimeter after the samples were purged with argon for 2 min. The spectra were not corrected for the photomultiplier spectral response.

Cyclic voltammetry was performed using a μAutolab III potentiostat/galvanostat (Autolab) using a standard three-electrode arrangement comprised of a glassy carbon working electrode (Metrohm), a Pt rod counter electrode (Metrohm) and a Ag wire as a pseudo-reference electrode. The experiments were performed in acetonitrile. TBAPF₆ (0.1 mol

L⁻¹) was added as the supporting electrolyte. The ferrocene/ferrocenium pair was used as the internal standard. Potentials were reported versus the normal hydrogen electrode (NHE) using E_{1/2} (Fc/Fc⁺) = 0.67 V vs. NHE at 298 K.^{55, 56}

Fabrication of the dye-sensitized solar cells

Solar cells were prepared in a sandwich-type arrangement using a modified previously described procedure.⁵⁷ The 3.2 mm FTO conducting glass plates were cleaned, immersed in a 40 mmol L⁻¹ aqueous TiCl₄ solution at 70 °C for 30 min and washed with water and ethanol. TiO₂ paste was deposited by screen-printing spots (A = 0.196 cm²) on the FTO glass, and heating at 125 °C for 6 min. This procedure was repeated 4 times. After the deposition, sintering process was performed by heating the TiO₂ films: 5 min at 325 °C, 5 min at 375 °C, 15 min at 450 °C and 15 min at 500 °C. This resulted in TiO₂ films with a 13.0 ± 0.7 μm thickness, as measured using a KLA-Tencor P-7 Stylus profiler. The films were sensitized by immersing TiO₂ electrodes into the ethanolic solution of the dye (~0.3 mmol L⁻¹) for 24 h. The counter-electrodes were prepared by depositing a hexachloroplatinic acid layer on the conductive side of a drilled conductive glass, followed by heating at 450 °C for 30 min. Solar cells were sealed using a film of sealant between the photoanode and counter-electrode, followed by heating to 110 °C using a custom-built sealing equipment. The mediator was placed between the photoanode and counter-electrode through the hole drilled on the counter-electrodes. The mediator was prepared by dissolving iodine (38 mg, 0.03 mol L⁻¹), guanidinium thiocyanate (59 mg, 0.1 mol L⁻¹), 4-*tert*-butylpyridine (0.38 mL, 0.5 mol L⁻¹) and 1-butyl-3-methylimidazolium iodide (0.80 g, 0.6 mol L⁻¹) in a mixture of acetonitrile:valeronitrile (85:15) to yield a 5 mL solution.

Photoelectrochemical measurements

Photocurrent action spectra and current-voltage curves were measured using a previously described Newport system.⁴³ The results of the presented photoelectrochemical experiments are the averages of, at least, four individual experiments.

RESULTS AND DISCUSSION

The FTIR spectrum of *cis*-[Ru(cbz₂-phen)(dcbH₂)(NCS)₂] as a neat solid exhibits peaks in the aromatic region, from 1650 to 1430 cm⁻¹, that are ascribed to ν_{C=C} and ν_{C-N} of the aromatic ligands, Figure 2. Additionally, aromatic C-H bending peaks are observed between 1275 and 1000 cm⁻¹.^{58, 59} Intense bands at 2107 cm⁻¹ and 754 cm⁻¹ are, respectively, ascribed to ν_{N-C} and ν_{C-S} and are characteristic of the NCS⁻ ligands that are coordinated through the nitrogen atom.^{60, 61} Thus, only the isothiocyanate isomer is obtained after purification. The distinct ν_{C=O} of the dcbH₂ protonated carboxylic groups can be observed at 1725 cm⁻¹. When adsorbed on the nanocrystalline mesoscopic TiO₂ film, *cis*-[Ru(cbz₂-phen)(dcbH₂)(NCS)₂] exhibits similar FTIR spectra, Figure 2, except for the absence of the

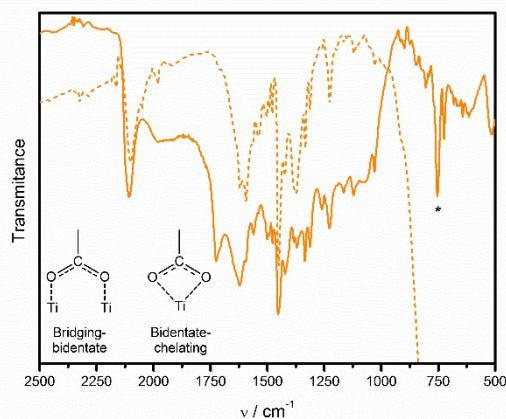


Figure 2. FTIR spectrum of *cis*-[Ru(cbz₂-phen)(dcbH₂)(NCS)₂] in KBr (—) and the ATR-FTIR spectrum of *cis*-[Ru(cbz₂-phen)(dcbH₂)(NCS)₂] that is adsorbed on the TiO₂ film (---). (* indicates the peak ascribed to the -NCS ligand at 754 cm⁻¹; Inset: binding modes of the dye on the TiO₂ surface).

$\nu_{C=O}$ peak near 1700 cm⁻¹ due to the formation of ester bonding. This indicates that the two carboxylic acid groups are completely anchored on the TiO₂ surface with a carboxylate COO⁻ bidentate coordination. The bands at 1620 cm⁻¹ and 1374 cm⁻¹ are ascribed to asymmetric and symmetric vibrations of the carboxylate groups, respectively. This confirms the bidentate or bridging chelating mode of adsorption of the complexes on the TiO₂ surface.⁶²

In the UV region, *cis*-[Ru(cbz₂-phen)(dcbH₂)(NCS)₂] exhibits intense absorption bands at approximately 330 and 310 nm, Figure 3, which are ascribed to intraligand π - π^* transitions of the cbz₂-phen and dcbH₂ ligands. The electronic spectrum of *cis*-[Ru(cbz₂-phen)(dcbH₂)(NCS)₂] exhibits two broad and intense MLCT absorption bands with a maxima at 375 nm (1.4×10^4 L mol⁻¹ cm⁻¹) and 525 nm (1.8×10^4 L mol⁻¹ cm⁻¹) assigned to MLCT transitions and are responsible for the high sunlight harvesting by this compound. This has been previously described in the literature for similar compounds.^{41, 42} Particularly, the 375 nm absorption band have a contribution of the cbz₂-phen ligand, since the cbz₂-phen compound itself also absorbs in this region.

Molar absorptivities determined for this compound are higher than those determined for *cis*-[Ru(phen)(dcbH₂)(NCS)₂], Figure S6 ($\epsilon_{425nm} = 1.1 \times 10^4$ L mol⁻¹ cm⁻¹ and $\epsilon_{525nm} = 1.0 \times 10^4$ L mol⁻¹ cm⁻¹) at almost all wavelengths in the 250-800 nm range due to the existence of the π -conjugated carbazole group at the 4 and 7 positions of the phenanthroline ring. This increases the molar absorptivity of this compound, as was observed for similar π conjugated groups.^{23, 48-50}

TiO₂ sensitization process was monitored up to 24 h by recording absorption changes on the semiconductor films, Figure S7. These absorption changes occur due to the increase in dye loading, which is responsible for sensitization. It is important to notice the absence of shifts on the absorption

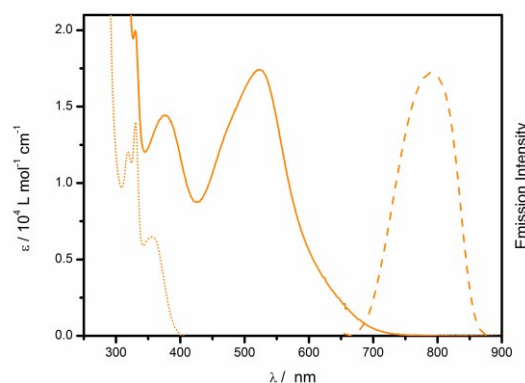


Figure 3. Absorption spectrum of *cis*-[Ru(cbz₂-phen)(dcbH₂)(NCS)₂] (—) and cbz₂-phen (···) in ethanol and the emission spectrum of *cis*-[Ru(cbz₂-phen)(dcbH₂)(NCS)₂] in acetonitrile at T = 298 K (---). ($\lambda_{ex} = 500$ nm; $\nu = 30$ nm min⁻¹).

maxima, which indicates that a dye monolayer was adsorbed on TiO₂.⁴⁸

The emission spectrum of *cis*-[Ru(cbz₂-phen)(dcbH₂)(NCS)₂] in acetonitrile, Figure 3, is broad and non-structured. It is typical of the ³MLCT lowest lying excited state of ruthenium polypyridyl compounds⁶⁰ and exhibits an emission maximum at 790 nm. The estimated HOMO-LUMO energy gap for the compound, E_{0-0} , is 1.86 eV. The gap is determined at the emission spectrum onset. Its emission maximum has a hypsochromic shift of 10 nm in comparison to *cis*-[Ru(phen)(dcbH₂)(NCS)₂].⁴⁴ It is known that in *cis*-[Ru(L-phen)(dcbH₂)(NCS)₂] dyes, the shifts in emission maxima are primarily ascribed to the differences in HOMO energies. Because *cis*-[Ru(Ph₂-phen)(dcbH₂)(NCS)₂] exhibits an emission energy higher than *cis*-[Ru(phen)(dcbH₂)(NCS)₂] due its lower HOMO energy,⁴³ the same trend on HOMO energy is expected for *cis*-[Ru(cbz₂-phen)(dcbH₂)(NCS)₂]. Electrochemical experiments were performed to evaluate the HOMO energy of the compound.

The cyclic voltammogram of *cis*-[Ru(cbz₂-phen)(dcbH₂)(NCS)₂], Figure 4, exhibits a *quasi*-reversible ground state electrochemical process for the ruthenium(II/III) wave at $E_{1/2} = 1.07$ V vs. NHE. This positive shift in comparison to *cis*-[Ru(phen)(dcbH₂)(NCS)₂] (1.05 V vs. NHE)⁴⁴ suggests that the presence of carbazole at the 4 and 7 positions of the phenanthroline ring decreases the electronic density at the metal center. In addition, two reduction peaks are observed at -1.09 V and -1.56 V vs. NHE and are ascribed to electrochemical processes on the ligands. The more positive reduction potential is ascribed to the dcbH₂ ligand due its lower LUMO levels.⁴¹

The excited state oxidation potential of this compound, $E(S^+/S^*) = -0.79$ V vs. NHE was determined using the equation $E(S^+/S^*) = E_{1/2}(S/S^+) - E_{0-0}$,⁴¹ where $E_{1/2}(S/S^+)$ is the ground state oxidation potential determined by cyclic voltammetry.

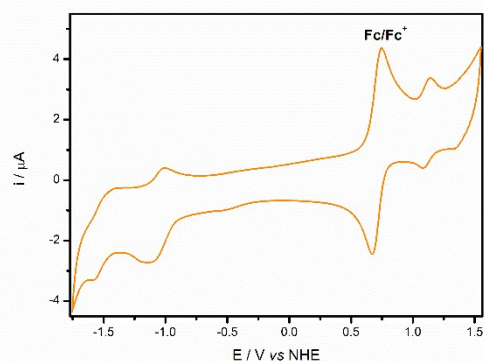


Figure 4. Cyclic voltammogram of *cis*-[Ru(cbz₂-phen)(dcbH₂)(NCS)₂] in acetonitrile at 298 K ($\nu = 100 \text{ mV s}^{-1}$; [TBAPF₆] = 0.1 mol L⁻¹).

The determined emission and electrochemical parameters are summarized in Table 1 and are compared to those determined for *cis*-[Ru(phen)(dcbH₂)(NCS)₂].⁴⁴

The $E(S^+/S^*)$ of *cis*-[Ru(cbz₂-phen)(dcbH₂)(NCS)₂] is more negative than the conduction band edge of TiO₂ anatase ($E_{CB} = -0.4 \text{ V vs. NHE at pH=4}$),^{63, 64} and its ground state oxidation potential is more positive than the I₂^{-•}/I⁻ (+0.93 V vs. NHE)⁶⁵ redox pair. These energies are adequate for using the dye in dye-sensitized solar cells because the energies allow electron injection from the excited state of the complex into the conduction band of TiO₂. Thermodynamically, its subsequent regeneration by the redox pair is favorable, as seen in the proposed energy diagram, Figure 5.

Table 1. Emission maxima wavelength (λ_{em}), estimated HOMO-LUMO energy gaps ($E_{0,0}$), ground state oxidation potentials [$E_{1/2}(S^+/S)$], and excited state oxidation potentials [$E(S^+/S^*)$] for *cis*-[Ru(cbz₂-phen)(dcbH₂)(NCS)₂] and *cis*-[Ru(phen)(dcbH₂)(NCS)₂].⁴⁴

Sensitizer	λ_{em} / nm	$E_{0,0} / \text{eV}$	$E_{1/2}(S^+/S) / \text{V vs. NHE}$	$E(S^+/S^*) / \text{V vs. NHE}$
<i>cis</i> -[Ru(cbz ₂ -phen)(dcbH ₂)(NCS) ₂]	790	1.86	+1.07	-0.79
<i>cis</i> -[Ru(phen)(dcbH ₂)(NCS) ₂]	800	1.90	+1.05	-0.85

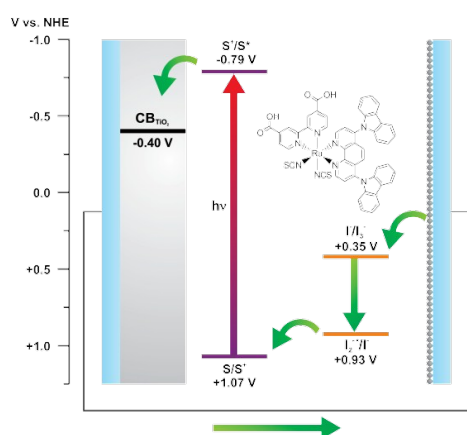


Figure 5. Energy diagram and schematic representation of some electron transfer processes that occur in a DSSC that uses a *cis*-[Ru(cbz₂-phen)(dcbH₂)(NCS)₂] dye-sensitizer.

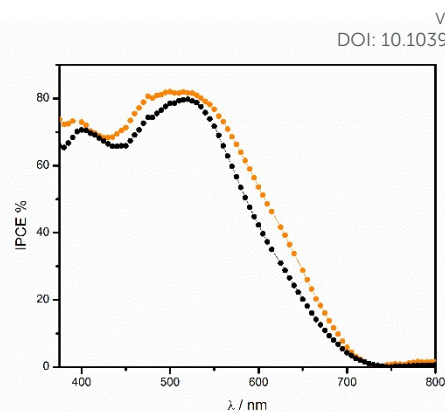


Figure 6. Photocurrent action spectra of solar cells that were sensitized by *cis*-[Ru(cbz₂-phen)(dcbH₂)(NCS)₂] (—○—) or N3 (—■—).

Dye-sensitized solar cells were characterized using the photocurrent action spectra and current-voltage curves. The photocurrent action spectrum of *cis*-[Ru(cbz₂-phen)(dcbH₂)(NCS)₂], Figure 6, resembles the absorption spectrum of its photoanode and shows that this compound has high efficiency for harvesting sunlight and converting it into electrical energy for the major part of visible spectrum. Its spectral features are similar to those determined for N3. However, its IPCE values are slightly higher in all the spectrum. Over the 370-800 nm spectral range, the integrated IPCE response for *cis*-[Ru(cbz₂-phen)(dcbH₂)(NCS)₂] was approximately 5.2% higher compared with the values for the sensitized by N3 solar cells under the same experimental conditions. This suggests that these solar cells have a more efficient photocurrent generation.

The overall performance of DSSCs under the simulated solar spectrum was evaluated using the current-voltage curves, Figure 7, and using the photovoltaic performance data for *cis*-[Ru(cbz₂-phen)(dcbH₂)(NCS)₂] and N3 as sensitizers on nanocrystalline TiO₂ solar cells, Table 2. As expected, based on the photocurrent action spectra, a higher J_{SC} was determined for the devices sensitized with *cis*-[Ru(cbz₂-phen)(dcbH₂)(NCS)₂] in comparison with the N3-sensitized devices. In addition, the higher V_{OC} determined also contributes for enhancing device efficiencies in comparison with those sensitized by N3. These differences cause *cis*-[Ru(cbz₂-phen)(dcbH₂)(NCS)₂] to surpass the efficiency values both of N3 as a dye-sensitizer for nanocrystalline TiO₂ cells and other ruthenium(II) *tris*-heteroleptic dyes that contain ligands of phenanthroline derivatives.⁴¹⁻⁴⁵

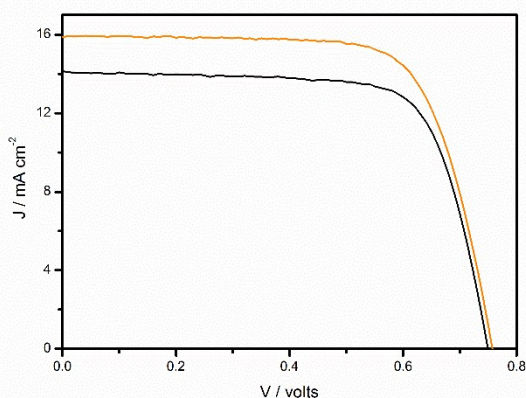


Figure 7. Current-voltage curves measured for solar cells sensitized using *cis*-[Ru(cbz₂-phen)(dcbH₂)(NCS)₂] (–) or N3 (–) under A.M. 1.5G irradiation ($P_{irr} = 100 \text{ mW cm}^{-2}$).

Table 2. Photoelectrochemical parameters determined for *cis*-[Ru(R₂-phen)(dcbH₂)(NCS)₂], R = cbz or H and for N3.

	R = cbz	R = H ⁴³	N3
V_{oc} / Volts	0.76 ± 0.01	0.733	0.75 ± 0.01
J_{sc} / mA cm ⁻²	15.6 ± 0.7	8.67	14.4 ± 0.3
η / %	8.6 ± 0.2	3.78	7.9 ± 0.2
P_{max} / mW cm ⁻²	8.5 ± 0.2	3.88	7.8 ± 0.2
Fill factor (ff)	0.716 ± 0.004		0.72 ± 0.01
IPCE (λ_{max}) / %	79 ± 3 (500)	56 (485)	77 ± 3 (520)

The devices sensitized using *cis*-[Ru(cbz₂-phen)(dcbH₂)(NCS)₂] exhibited a higher performance compared with the unsubstituted phenanthroline dye, *cis*-[Ru(phen)(dcbH₂)(NCS)₂].^{38, 43} This can be explained using the thermodynamic data and chemical structure of the compound. The $E_{S^+_{1/2}}$ is sufficiently negative to promote electron injection into the TiO₂ conduction band via either the hot singlet excited state or triplet excited states. In addition, $E_{S^+_{1/2}}$ is more positive than what was determined for similar reported compounds,^{43, 44} and it is more positive than $E_{1/2}^{-1/1}$. This results in a fast and more efficient dye-regeneration by the mediator, which is required for high-performance devices. Due to $E_{S^+_{1/2}}$ and $E_{S^+_{1/2}}$ values, the thermodynamics of *cis*-[Ru(cbz₂-phen)(dcbH₂)(NCS)₂] dye is favorable for solar energy conversion using DSSCs. It is important to highlight that carbazole groups at the 4 and 7 positions of phenanthroline play an important role in electron injection dynamics. These groups have a delocalized π electron cloud, and the dihedral angle between the phenanthroline and carbazole subunits is decreased in the excited state.⁶⁶ Furthermore, the increase in coplanarity was reported for ruthenium(II) compounds that have phenyl substituents on phenanthroline⁶⁷ or in bipyridine^{68, 69} ligands. The increase in coplanarity results in a more delocalized system, that increases the triplet excited state lifetime. For *cis*-[Ru(cbz₂-phen)(dcbH₂)(NCS)₂], this process probably occurs, and electron injection via the triplet pathway plays an important role in the energy conversion efficiency.

CONCLUSIONS

View Article Online

DOI: 10.1039/C6RA08666G

The novel *tris*-heteroleptic ruthenium(II) dye, *cis*-[Ru(cbz₂-phen)(dcbH₂)(NCS)₂], was synthesized, characterized and applied as a sensitizer in DSSCs. Its absorption spectrum overlaps with the visible spectrum and also has high molar absorptivity MLCT bands. The adequate energy levels make *cis*-[Ru(cbz₂-phen)(dcbH₂)(NCS)₂] suitable for the use as a dye-sensitizer in photovoltaic devices. The sensitization of TiO₂ with *cis*-[Ru(cbz₂-phen)(dcbH₂)(NCS)₂] led to solar cells that surpassed the efficiency of both N3 and other published ruthenium(II) *tris*-heteroleptic that contain phenanthroline derivative ligands, as a dye-sensitizers for nanocrystalline TiO₂ solar cells. The improved observed efficiency is attributed to carbazole groups that are capable of changing energy levels of the dye, which results in thermodynamically favorable electron injection and dye regeneration processes. Additionally, these groups can increase the triplet lifetime due to higher π electron delocalization on this excited state, which favors a higher contribution for electron injection via the triplet pathway. The use of electron delocalized groups at the 4 and 7 positions of phenanthroline is a promising alternative in the molecular design of new ruthenium(II) polypyridyl dye-sensitizers.

Acknowledgements

The authors are grateful to CAPES and to Fundação de Amparo à Pesquisa do Estado de São Paulo (FAPESP) for the financial support (2013/25173-5, 2015/00605-5, 2015/13149-8 and 2015/21110-4).

References

1. M. Grätzel, *J. Photochem. Photobiol. C-Photochem. Rev.*, 2003, **4**, 145-153.
2. J. Yang, K. Kim, C. Bark and H. Choi, *Nanoscale Research Letters*, 2014, **9**, 671.
3. B. Oregan and M. Gratzel, *Nature*, 1991, **353**, 737-740.
4. A. Hagfeldt and M. Gratzel, *Acc. Chem. Res.*, 2000, **33**, 269-277.
5. A. Kay and M. Grätzel, *Sol. Energy Mater. Sol. Cells*, 1996, **44**, 99-117.
6. G. Smestad, C. Bignozzi and R. Argazzi, *Sol. Energy Mater. Sol. Cells*, 1994, **32**, 259-272.
7. M. Grätzel, *Phil. Trans. R. Soc. A*, 2007, **365**, 993-1005.
8. J. Navas, C. Fernández-Lorenzo, T. Aguilar, R. Alcántara and J. Martín-Calleja, *Phys. Status Solidi A*, 2012, **209**, 378-385.
9. S. A. Mozaffari, M. Ranjbar, E. Kouhestanian, H. S. Amoli and M. H. Armanmehr, *Mater. Sci. Semicond. Process.*, 2015, **40**, 285-292.
10. T. Aguilar, J. Navas, R. Alcántara, C. Fernandez-Lorenzo, G. Blanco, A. Sanchez-Coronilla and J. Martín-Calleja, *Appl. Phys. A-Mater. Sci. Process.*, 2015, **121**, 1261-1269.
11. A. R. Tanyi, A. I. Rafieh, P. Ekaneyaka, A. L. Tan, D. J. Young, Z. Zheng, C. Vijila, G. S. Subramanian and R. L. N. Chandrakanthi, *Electrochim. Acta*, 2015, **178**, 240-248.
12. S. R. Sun, L. Gao and Y. Q. Liu, *Appl. Phys. Lett.*, 2010, **96**, 3.
13. A. O. T. Patrocínio, L. G. Paterno and N. Y. Murakami Iha, *J. Photochem. Photobiol., A*, 2009, **205**, 23-27.

14. L. F. Paula, R. C. Amaral, N. Y. Murakami Iha, R. M. Paniago, A. E. H. Machado and A. O. T. Patrocínio, *RSC Advances*, 2014, **4**, 10310-10316.
15. S. A. Sapp, C. M. Elliott, C. Contado, S. Caramori and C. A. Bignozzi, *J. Am. Chem. Soc.*, 2002, **124**, 11215-11222.
16. H. Nusbaumer, J. E. Moser, S. M. Zakeeruddin, M. K. Nazeeruddin and M. Grätzel, *J. Phys. Chem. B*, 2001, **105**, 10461-10464.
17. S. Yanagida, Y. H. Yu and K. Manseki, *Acc. Chem. Res.*, 2009, **42**, 1827-1838.
18. D. K. Lee, K. S. Ahn, S. Thogiti and J. H. Kim, *Dyes Pigm.*, 2015, **117**, 83-91.
19. A. Apostolopoulou, M. Vlasίου, P. A. Tziouris, C. Tsiafoulis, A. C. Tspis, D. Rehder, T. A. Kabanos, A. D. Keramidas and E. Stathatos, *Inorg. Chem.*, 2015, **54**, 3979-3988.
20. L. Tao, Z. Huo, Y. Ding, Y. Li, S. Dai, L. Wang, J. Zhu, X. Pan, B. Zhang, J. Yao, M. K. Nazeeruddin and M. Grätzel, *J. Mater. Chem A*, 2015, **3**, 2344-2352.
21. K. Hara, T. Sato, R. Katoh, A. Furube, T. Yoshihara, M. Murai, M. Kurashige, S. Ito, A. Shinpo, S. Suga and H. Arakawa, *Adv. Funct. Mater.*, 2005, **15**, 246-252.
22. K. Hara, Z. S. Wang, T. Sato, A. Furube, R. Katoh, H. Sugihara, Y. Dan-Oh, C. Kasada, A. Shinpo and S. Suga, *J. Phys. Chem. B*, 2005, **109**, 15476-15482.
23. Z. S. Wang, N. Koumura, Y. Cui, M. Takahashi, H. Sekiguchi, A. Mori, T. Kubo, A. Furube and K. Hara, *Chem. Mater.*, 2008, **20**, 3993-4003.
24. J. Y. Mao, X. Y. Zhang, S. H. Liu, Z. J. Shen, X. Li, W. J. Wu, P. T. Chou and J. L. Hua, *Electrochim. Acta*, 2015, **179**, 179-186.
25. S. Mathew, A. Yella, P. Gao, R. Humphry-Baker, F. E. Curchod, N. Ashari-Astani, I. Tavernelli, U. Rothlisberger, K. Nazeeruddin and M. Grätzel, *Nat Chem*, 2014, **6**, 242-247.
26. J.-S. Ni, K.-C. Ho and K.-F. Lin, *J. Mater. Chem A*, 2013, **1**, 3463-3470.
27. K. Cao, J. Lu, J. Cui, Y. Shen, W. Chen, G. Alemu, Z. Wang, H. Yuan, J. Xu, M. Wang and Y. Cheng, *J. Mater. Chem A*, 2014, **2**, 4945-4953.
28. W.-C. Chang, C. Su, S.-Y. Ho, K. Prabakaran, Y. S. Tingare, C.-Y. Li, T.-Y. Li, S.-H. Tsai and W.-R. Li, *J. Mater. Chem A*, 2013, **1**, 8716-8720.
29. P.-Y. Ho, C.-H. Siu, W.-H. Yu, P. Zhou, T. Chen, C.-L. Ho, L. T. L. Lee, Y.-H. Feng, J. Liu, K. Han, Y. H. Lo and W.-Y. Wong, *J. Mater. Chem. C*, 2016, **4**, 713-726.
30. D. Demeter, J. Roncali, S. Jungstittiwong, F. Melchiorre, P. Biagini and R. Po, *J. Mater. Chem. C*, 2015, **3**, 7756-7761.
31. P. Wang, S. M. Zakeeruddin, J. E. Moser, M. K. Nazeeruddin, T. Sekiguchi and M. Grätzel, *Nat Mater*, 2003, **2**, 402-407.
32. C. Sahin, C. Tozlu, K. Ocaoglu, C. Zafer, C. Varlikli and S. Icli, *Inorg. Chim. Acta*, 2008, **361**, 671-676.
33. M. K. Nazeeruddin, S. M. Zakeeruddin, J. J. Lagref, P. Liska, P. Comte, C. Barolo, G. Viscardi, K. Schenk and M. Graetzel, *Coord. Chem. Rev.*, 2004, **248**, 1317-1328.
34. C. Klein, M. K. Nazeeruddin, D. Di Censo, P. Liska and M. Grätzel, *Inorg. Chem.*, 2004, **43**, 4216-4226.
35. M. K. Nazeeruddin, T. Bessho, L. Cevey, S. Ito, C. Klein, F. De Angelis, S. Fantacci, P. Comte, P. Liska, H. Imai and M. Graetzel, *J. Photochem. Photobiol., A*, 2007, **185**, 331-337.
36. J. d. S. de Souza, L. O. M. de Andrade and A. S. Polo, in *Nanoenergy*, eds. F. L. de Souza and E. R. Leite, Springer Berlin Heidelberg, 2013, DOI: 10.1007/978-3-642-31736-1_2, ch. 2, pp. 49-80.
37. K. Hara, H. Sugihara, Y. Tachibana, A. Islam, M. Yanagida, K. Sayama, H. Arakawa, G. Fujihashi, T. Horiguchi and T. Kinoshita, *Langmuir*, 2001, **17**, 5992-5999.
38. N. Onozawa-Komatsuzaki, O. Kitao, M. Yanagida, Y. Himeda, H. Sugihara and K. Kasuga, *New J. Chem.*, 2006, **30**, 689-697.
39. C. Y. Chen, H. C. Lu, C. G. Wu, J. G. Chen and K. C. Ho, *Adv. Funct. Mater.*, 2007, **17**, 29-36.
40. A. Reynal, A. Forneli, E. Martinez-Ferrero, A. Sanchez-Diaz, A. Vidal-Ferran and E. Palomares, *Eur. J. Inorg. Chem.*, 2008, DOI: 10.1002/ejic.200800054, 1955-1958.
41. Y. L. Sun, A. C. Onicha, M. Myahkostupov and F. N. Castellano, *ACS Appl. Mat. Inter.*, 2010, **2**, 2039-2045.
42. A. O. Adeloye, *Molecules*, 2011, **16**, 8353-8367.
43. F. Carvalho, E. Liandra-Salvador, F. Bettanin, J. S. Souza, P. Homem-de-Mello and A. S. Polo, *Inorg. Chim. Acta*, 2014, **414**, 145-152.
44. A. V. Müller, P. S. Mendonça, S. Parant, T. Duchanois, P. C. Gros, M. Beley and A. S. Polo, *J. Braz. Chem. Soc.*, 2015, **26**, 2224-2232.
45. A. Reynal, A. Forneli, E. Martinez-Ferrero, A. Sanchez-Diaz, A. Vidal-Ferran and E. Palomares, *Eur. J. Inorg. Chem.*, 2008, **2008**, 1955-1958.
46. A. Reynal, A. Forneli, E. Martinez-Ferrero, A. Sánchez-Díaz, A. Vidal-Ferran, B. C. O'Regan and E. Palomares, *J. Am. Chem. Soc.*, 2008, **130**, 13558-13567.
47. M. Miyashita, K. Sunahara, T. Nishikawa, Y. Uemura, N. Koumura, K. Hara, A. Mori, T. Abe, E. Suzuki and S. Mori, *J. Am. Chem. Soc.*, 2008, **130**, 17874-17881.
48. S.-J. Wu, C.-Y. Chen, J.-Y. Li, J.-G. Chen, K.-M. Lee, K.-C. Ho and C.-G. Wut, *J. Chin. Chem. Soc.*, 2010, **57**, 1127-1130.
49. C.-Y. Chen, N. Pootrakulchote, S.-J. Wu, M. Wang, J.-Y. Li, J.-H. Tsai, C.-G. Wu, S. M. Zakeeruddin and M. Grätzel, *J. Phys. Chem. C*, 2009, **113**, 20752-20757.
50. C.-Y. Chen, N. Pootrakulchote, T.-H. Hung, C.-J. Tan, H.-H. Tsai, S. M. Zakeeruddin, C.-G. Wu and M. Grätzel, *J. Phys. Chem. C*, 2011, **115**, 20043-20050.
51. C. L. Donnici, D. H. Maximo, L. L. C. Moreira, G. T. dos Reis, E. F. Cordeiro, I. M. F. de Oliveira, S. Carvalho and E. B. Paniago, *J. Braz. Chem. Soc.*, 1998, **9**, 455-460.
52. G. G. Shan, H. B. Li, H. T. Cao, D. X. Zhu, Z. M. Su and Y. Liao, *J. Organomet. Chem.*, 2012, **713**, 20-26.
53. Z. Q. Gao, M. Luo, X. H. Sun, H. L. Tam, M. S. Wong, B. X. Mi, P. F. Xia, K. W. Cheah and C. H. Chen, *Advanc Mat*, 2009, **21**, 688+.
54. G. Zucchi, V. Murugesan, D. Tondelier, D. Aldakov, T. Jeon, F. Yang, P. Thuéry, M. Ephritikhine and B. Geffroy, *Inorg. Chem.*, 2011, **50**, 4851-4856.
55. N. G. Connelly and W. E. Geiger, *Chem. Rev.*, 1996, **96**, 877-910.
56. R. H. Crabtree, *Energy Production and Storage: Inorganic Chemical Strategies for a Warming World*, Wiley, 2013.
57. S. Ito, T. N. Murakami, P. Comte, P. Liska, C. Grätzel, M. K. Nazeeruddin and M. Grätzel, *Thin Solid Films*, 2008, **516**, 4613-4619.
58. B. H. Stuart, *Infrared Spectroscopy: Fundamentals and Applications*, Wiley, 2004.
59. R. M. Silverstein, F. X. Webster, D. Kiemle and D. L. Bryce, *Spectrometric Identification of Organic Compounds, 8th Edition*, Wiley, 2014.
60. M. K. Nazeeruddin, S. M. Zakeeruddin, R. Humphry-Baker, M. Jirousek, P. Liska, N. Vlachopoulos, V. Shklover, C.-H. Fischer and M. Grätzel, *Inorg. Chem.*, 1999, **38**, 6298-6305.
61. M. K. Nazeeruddin, A. Kay, I. Rodicio, R. Humphry-Baker, E. Müller, P. Liska, N. Vlachopoulos and M. Grätzel, *J. Am. Chem. Soc.*, 1993, **115**, 6382-6390.
62. K. Kilså, E. I. Mayo, B. S. Brunschwig, H. B. Gray, N. S. Lewis and J. R. Winkler, *J. Phys. Chem. B*, 2004, **108**, 15640-15651.
63. A. Hagfeldt and M. Graetzel, *Chem. Rev.*, 1995, **95**, 49-68.
64. K. Kalyanasundaram and M. Grätzel, *Coord. Chem. Rev.*, 1998, **177**, 347-414.
65. G. Boschloo and A. Hagfeldt, *Acc. Chem. Res.*, 2009, **42**, 1819-1826.
66. N. D. McClenaghan, R. Passalacqua, F. Loiseau, S. Campagna, B. Verheyde, A. Hameurlaine and W. Dehaen, *J. Am. Chem. Soc.*, 2003, **125**, 5356-5365.

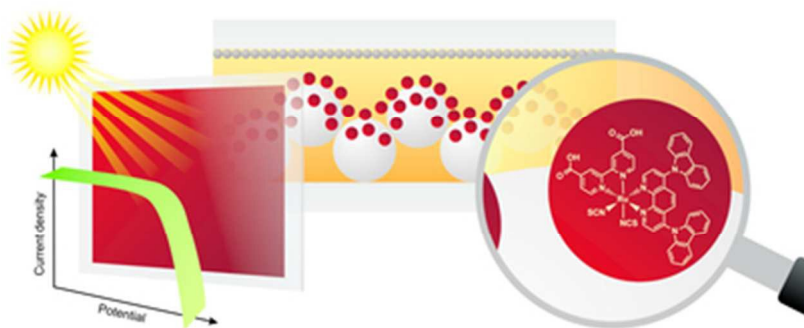
ARTICLE

RSC Adv.

67. F. Liu and G. J. Meyer, *Inorg. Chem.*, 2005, **44**, 9305-9313.
68. N. H. Damrauer, T. R. Boussie, M. Devenney and J. K. McCusker, *J. Am. Chem. Soc.*, 1997, **119**, 8253-8268.
69. A. E. Curtright and J. K. McCusker, *J. Phys. Chem. A*, 1999, **103**, 7032-7041.

View Article Online
DOI: 10.1039/C6RA08666G

RSC Advances Accepted Manuscript



34x14mm (300 x 300 DPI)